various possible structures in relatively concentrated polysilicate solutions.

Acknowledgment. We wish to thank Mr. Steven Daniels, an Oak Ridge Associated Universities Summer Trainee in 1976, for assistance with some of the experimental observations. Research was sponsored by the Division of Physical Research of the Energy Research and Development Administration under contract with Union Carbide Corp.

Registry No. Si(OH)$_4$, 10193-36-9; SiO(OH)$_3^-$, 18102-72-2; SiO$_2$(OH)$_2^{2-}$, 27831-51-2; Si$_4$(OH)$_{18}^{2-}$, 63588-54-5.

References and Notes

(1) T. M. Seward, *Geochim. Cosmochim. Acta*, **38**, 1651 (1974).
(2) B. N. Ryzhenko, *Geochem. Int.*, **4**, 99 (1967).
(3) D. Fortnum and J. O. Edwards, *J. Inorg. Nucl. Chem.*, **11**, 264 (1955).
(4) J. E. Earley, D. Fortnum, A. Wojcicki, and J. O. Edwards, *J. Am. Chem. Soc.*, **81**, 1295 (1959).
(5) E. Freund, *Bull. Soc. Chim. Fr.*, **7-8**, 2238, 2244 (1973).
(6) H. Bilinski and N. Ingri, *Acta Chem. Scand.*, **21**, 2503 (1967).
(7) K. A. Fanning and M. E. Q. Pilson, *Anal. Chem.*, **45**, 136 (1973).
(8) N. Ingri, *Acta Chem. Scand.*, **13**, 758 (1959).
(9) J. Aveston, *J. Chem. Soc.*, 4444 (1965).
(10) R. E. Mesmer, C. F. Baes, Jr., and F. H. Sweeton, *J. Phys. Chem.*, **74**, 1937 (1970).
(11) A. S. Quist and W. L. Marshall, *J. Phys. Chem.*, **69**, 2984 (1965).
(12) R. E. Mesmer and C. F. Baes, Jr., *J. Solution Chem.*, **3**, 307 (1974).
(13) R. E. Mesmer, C. F. Baes, Jr., and F. H. Sweeton, *Inorg. Chem.*, **11**, 537 (1972).
(14) R. H. Busey and R. E. Mesmer, *J. Solution Chem.*, **5**, 147 (1976).
(15) R. M. Rush, J. S. Johnson, and K. A. Kraus, Report ORNL-3278, Oak Ridge National Laboratory, Oak Ridge, Tenn., 1963.
(16) A. F. Wells, "Structural Inorganic Chemistry", 4th ed, Clarendon Press, Oxford, 1975.
(17) K. S. Pitzer, *J. Phys. Chem.*, **77**, 268 (1973).
(18) J. W. Cobble, *J. Am. Chem. Soc.*, **86**, 5394 (1964).
(19) A. G. Volosov, I. L. Khodakowskiy, and B. N. Ryzhenko, *Geochem. Int.*, **9**, 362 (1972).
(20) D. A. Crerar and G. M. Anderson, *Chem. Geol.*, **8**, 107 (1971).
(21) J. Vilim, *Collect. Czech. Chem. Commun.*, **26**, 1268 (1961).
(22) J. A. Van Lier, P. L. de Bruyn, and J. T. G. Overbeek, *J. Phys. Chem.*, **64**, 1675 (1960).
(23) S. A. Greenburg, *J. Am. Chem. Soc.*, **80**, 6508 (1958).
(24) S. A. Greenberg and E. W. Price, *J. Phys. Chem.*, **61**, 1539 (1957).
(25) R. Schwarz and W. D. Müller, *Z. Anorg. Allg. Chem.*, **296**, 273 (1958).
(26) B. N. Ryzhenko and N. I. Khitarov, *Geokhimiya*, **8**, 957 (1968).
(27) G. Lagerström, *Acta Chem. Scand.*, **13**, 722 (1959).

Contribution from Argonne National Laboratory,
Chemistry Division, Argonne, Illinois 60439

Sputtered Gold and Silver Atoms Isolated in D_2, Ne, and N_2 Matrices[1]

D. M. GRUEN and J. K. BATES*

Received April 17, 1977 AIC70279H

The spectra of sputtered gold and silver atoms isolated in D_2, Ne, and N_2 matrices are reported. An inverse relationship between Z_{eff} of the metal atom and α, the polarizability of the matrix, has been extended to include silver atoms in D_2 and N_2 matrices. The correlation breaks down for Ne matrices apparently because the size of a substitutional site and polarizability of neon are such as to cause multiple-site occupation. Evidence for multiple-site occupation of silver in neon is presented. Intense and resolved spectra of silver dimers are also reported, and a correlation with the gas-phase spectra is made.

Introduction

The spectra of matrix-isolated gold[2,3] and silver[3b-9] atoms have been extensively studied and the main spectral features of both species are well characterized. The ground state of both atoms is ^2S giving rise to a relatively simple absorption spectrum in the ultraviolet region, corresponding to the lowest lying P → S transition with the ^2P state split by spin–orbit coupling. The matrix spectra, which generally consist of three absorptions, have been correlated with the spectrum of the gas-phase atomic species by postulating a perturbation of the atomic energy levels by the matrix cage.

Specifically, in the matrix the orbital degeneracy of the $^2P_{3/2}$ level is removed by a crystal field effect, yielding two sublevels, $P_{3/2\pm1/2}$ and $P_{3/2\pm3/2}$. Previous work with matrix-isolated gold atoms[3a] has correlated the variance of the spin–orbit coupling constant, ζ, in Ar, Kr, and Xe matrices with an increase in Z_{eff} of the gold nucleus. The electronic charge density of the 6p electron is increased by compression of the 6p wave function due to the repulsive interaction between the Au atom and the noble gas cage.[3a] The amount of compression depends on site considerations of the isolated gold atoms, the polarizability of the matrix atoms, and the temperature at which the matrix is observed.

When, as is the case for gold atoms isolated in Ar, Kr, and Xe matrices, the substitutional sites have the same symmetry properties, there exists a linear relationship between polarizability α of the matrix and Z_{eff}. ESR studies[10] of gold atoms isolated in Ar, Kr, and Xe matrices are in agreement with optical results indicating a single substitutional site and both the hyperfine and spin–orbit coupling constants increase as the matrix atoms become lighter and less polarizable. However, in neon matrices the ESR studies indicate that gold atoms occupy at least two different sites, and the value of the hyperfine coupling constant, A, in neon is nearly the same as that in Kr. It was of interest, therefore, to see if the spin–orbit coupling constant of Au in Ne undergoes a similar reversal indicative of different site geometries in this matrix.

As a further test of the relationship between the magnitude of the spin–orbit coupling constant and matrix polarizability, it was decided to study silver atoms, whose van der Waals radius and thus matrix behavior should be similar to that of gold. While presently available ESR and optical results for silver atoms isolated in rare gas matrices indicate that the spin–orbit and hyperfine coupling constants show trends similar to gold atoms, there has been up to now no direct evidence for multiple-site occupation.

Thus, to determine the range of applicability of the relationship between matrix polarizability and Z_{eff} and to obtain additional data on multiple-site occupations, the optical spectra of gold and silver atoms in Ne, N_2, and D_2 matrices have been included in our studies.

Throughout this work metal atoms have been produced by sputtering from a metal surface. This method of metal atom production, with the proper experimental conditions, appears to be especially conducive to the formation of metal dimers in the matrix, at least in the case of silver. Dimer formation appears to occur during deposition at the surface or near-surface region of the matrix before the kinetic energy of the sputtered atoms can be dissipated. The energy of sputtered metal atoms is the order of 1–10 eV, which is considerably

Table I. Atomic Parameters for Au and Ag Isolated in Various Matrices[a]

	Gaseous atoms	Gold					
		Ar[b]	Kr[b]	Xe[b]	Ne	N_2	D_2
$E_1(^2P_{1/2})$	37359	39175	38288	36875	38900	38260	38010
$E_2(^2P_{3/2,1/2})$	41174	44375	43113	41090	43670	43160	43655
$E_3(^2P_{3/2,3/2})$	41174	43763	42475	40525	43280	42330	42360
ΔE_1	3815	5200	4825	4215	4770	4900	5645
ΔE_2	3815	4588	4187	3650	4380	4070	4350
ζ_1	2543	3263	3004	2622	3050	2990	3331
A_1		−612	−638	−565	−390	−830	−1195
ζ_2	2543	3230	2966	2588	3035	2928	3210
A_2		−580	−600	−531	−375	−769	−1166
α, Å^3		1.63	2.48	4.01	0.398	1.77	0.82
Z_{eff}		5.10	4.99	4.82	5.01	4.97	5.09

	Gaseous atoms	Silver					
		Ar[c]	Kr[c]	Xe[d]	Ne	N_2	D_2
$E_1(^2P_{1/2})$	29552	31749	30966	29940	(30817) (31300)	30560	30360
$E_2(^2P_{3/2,1/2})$	30473	33489	32328	30969	(32206) (32733)	32310	32680
$E_3(^2P_{3/2,3/2})$	30473	32908	31892	(30693) (30571)	(31898) (32310)	31645	31640
ΔE_1	921	1740	1362	1029	1411	1750	2320
ΔE_2	921	1159	926	692	1046	1085	1280
ζ_1	614	966	763	573	819	945	973
A_1		−581	−436	−337	−365	−665	−920
ζ_2	614	889	707	532	781	847	973
A_2		−504	−380	−294	−326	−567	−920
Z_{eff}		3.73	3.52	3.28	3.61	3.69	3.81

[a] All values except α and Z_{eff} are in units of cm^{-1}. [b] Reference 3a. [c] References 4, 6–8. [d] The Xe spectrum consists of four absorptions due to a Ag–Xe interaction; see ref 4.

larger than that of atoms produced with thermal sources. This results in greater mobility of the atoms before isolation thus providing ideal conditions for dimer formation.

While spectra of matrix-isolated silver dimers have been reported,[7,11,12] we have been able to obtain considerably more intense and therefore somewhat better resolved dimer spectra. The increased intensity and resolution, in turn, have allowed one to make more definitive assignments of the dimer transitions.

Experimental Section

The metal atoms are produced by sputtering a metal target with a beam of 2-keV argon ions produced with a sputter ion gun. The details of the apparatus are presented elsewhere.[2] Briefly, the ion beam is produced in a differentially pumped chamber and enters the matrix isolation Dewar through a small aperature. The ion beam then passes through a hole in a sapphire deposition plate and strikes a metal target, and the back-sputtered products are mixed with matrix gas and collected on a deposition plate. This arrangement allows the sputtering gas to differ from the matrix gas without overly contaminating the matrix. Argon is generally used as the sputtering gas as its sputtering yield, atoms produced/incident ion, is reasonably large and it is unreactive.

The sputtering process also allows a direct determination of the metal atom to matrix gas ratio, M/R, to be made.[3a] The sputtering yield of argon on most metals is known; thus with precise monitoring of the matrix gas flow rate, M/R may be calculated.[3a] With integrated currents of 1–10 μA h and matrix gas flow rates of 0.5–1.0 mm/h, M/R values of 500:1 to 10^4:1 are obtained in depositions ranging from 30 min to 1 h. The metal targets are 0.75-in. disks stamped from 10-mil foil, and before matrix deposition the target is sputter cleaned with argon. Neon and deuterium matrices are formed at 4.2 K using a liquid-helium cryostat while experiments with Ar and N_2 matrices were generally done at 13 K with a closed cycle He refrigerator. Neon and deuterium matrices were annealed at 10 and 7 K, respectively, while annealing of Ar and N_2 matrices was done at 20, 30, and 40 K.

After matrix formation the deposition plate is rotated 90° to allow spectroscopic observation using a Cary 17H spectrometer with direct computer interface. The matrices have also been irradiated with light from a B&L SP-200 mercury source, but no luminescence was observed.

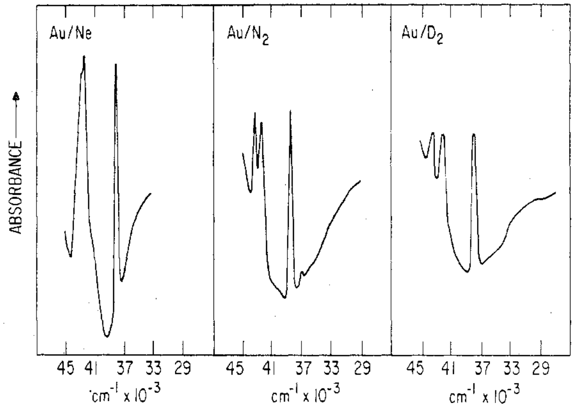

Figure 1. Ultraviolet absorption spectra of gold atoms isolated in Ne, N_2, and D_2 matrices.

Results and Discussion

Gold. The spectra of gold atoms isolated in Ne, N_2, and D_2 matrices are shown in Figure 1 and the relevant data are listed in Table I. The spin–orbit coupling and crystal field parameters have been calculated by two methods. In the first approximation the crystal field splitting, A_1, is equal to the separation between the $^2P_{3/2,3/2}$ and $^2P_{3/2,1/2}$ levels, while the spin–orbit coupling constant ζ_1 is calculated by averaging the $^2P_{3/2}$ components and taking the difference $^2P_{3/2}(av) - {}^2P_{1/2}$ as equal to $^3/_2\zeta_1$. More accurate values, A_2 and ζ_2, can be obtained by simultaneously diagonalizing the spin–orbit and crystal field interaction. The correct equations for ζ_2 and A_2 are

$$\zeta_2 = {}^1/_2(4\Delta E_2 - 2\Delta E_1) - A_2$$

and

$$A_2 = {}^1/_3(2\Delta E_2 - \Delta E_1) - [\Delta E_1{}^2 + 2\Delta E_2(\Delta E_1 - \Delta E_2)]^{1/2}$$

where the energy differences are defined as

$$\Delta E_1 = E_2 - E_3$$

$$\Delta E_2 = E_1 - E_3$$

Z_{eff} is obtained from the relationship

$$\Delta E(^2\mathrm{P}_{1/2} - {}^2\mathrm{P}_{3/2})\ \mathrm{cm}^{-1} = (3815.4/(4.8)^4)(Z_{\mathrm{eff}})^4$$

Of primary interest are the results for gold terms isolated in a neon matrix where the spin–orbit coupling constant is similar to its value for gold in Kr but considerably less than predicted on straightforward polarizability considerations. The smaller substitutional sites existing in a neon matrix presumably result in gold atoms in neon occupying multiple sites as shown by ESR measurement,[10] with perhaps one gold atom replacing two neon atoms in each site.

It should also be noted that the crystal field splitting in neon is substantially less negative than in Ar, Kr, or Xe. If this splitting, which is a reflection of the distortion of the lattice site symmetry, is a function $F(\alpha^x/r^y)$, the decrease could be due to the low value of α for neon or an increase in r which would exist if gold occupied a double substitutional site. Both factors acting in concert would produce the same results, of course.

The isolation of gold atoms in a nitrogen matrix is complicated by the appearance of two weak but quite sharp absorptions at 36 750 and 40 535 cm^{-1}. These bands are most easily observed after prolonged sputtering and on annealing decrease in intensity proportionally with the strong atomic absorptions. These features could be due to dimer or polymer formation, or site effects, but at this point have not been positively assigned. The average site size and polarizability for a nitrogen matrix are not too different from those of Kr and while the crystal field splitting which is sensitive to site symmetry has increased in N_2 as compared to Ar, Kr, and Xe, the spin–orbit coupling which is sensitive to polarizability and cage size is similar to that in Kr.

With deuterium, the only previously reported use of this matrix has been to study trapped water molecules.[13] A spectrum characteristic of gold atoms is observed in deuterium although the band intensity continuously decreases during observation, probably due to diffusion. No evidence for molecule formation, either gold dimers or gold deuteride, is observed.

The spin–orbit coupling and bandwidth in D_2 are comparable to those in Ar but the crystal field splitting is considerably larger than in noble gas or in N_2 matrices. Since the polarizability and site size for D_2 lie between Ne and Ar it appears that gold atoms in D_2 occupy highly distorted single sites. Deuterium, therefore, may represent the matrix with the smallest cage size and lowest polarizability which still allows substitutional site occupation by gold atoms.

The increase in spin–orbit coupling of Au in matrices was ascribed to a repulsive interaction between the Au atom and the matrix cage resulting in an increased charge density of the 6p electron wave function nearer the gold nucleus. The extent of compression of the 6p wave function can be monitored by determining Z_{eff} for gold in each matrix. As the polarizability of the matrix decreases, Z_{eff} increases, and this relationship is depicted in Figure 2a.

Although gold may be interacting with N_2, comparison with rare gas matrices is still possible since its atomic spectrum is preserved. It is clear that the general trend relating polarizability to Z_{eff} can be extended to N_2 and D_2 matrices. In the case of neon, where Z_{eff} is far smaller than expected from the general trend, the gold atom appears to occupy positions where the packing has relaxed, causing less compression of the 6p wave function and indicating a double substitutional site.

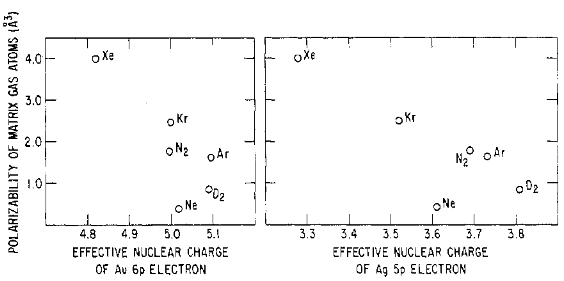

Figure 2. Matrix gas atom polarizabilities vs. Z_{eff} of the (a) Au 6p electron and (b) Ag 5p electron.

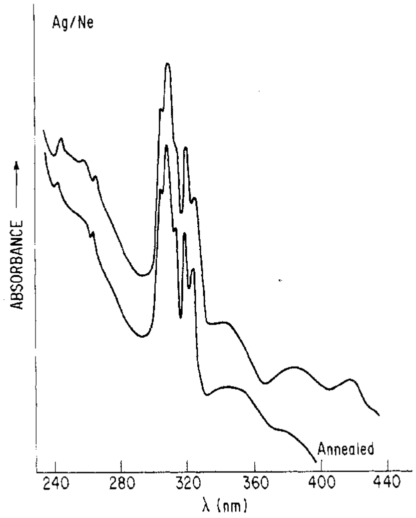

Figure 3. Absorption spectrum of silver atoms isolated in a Ne matrix.

Silver. Silver atoms have been isolated in Ne, N_2, and D_2 matrices and these results together with those tabulated for Ar, Kr, and Xe matrices are listed in Table I. The values for the $^2P_{3/2}$ and $^2P_{1/2}$ absorption in Ar, Kr, and Xe are taken from literature data[4,6,8] where the deposition temperature is 15 K or below. Above 15 K the temperature dependence of A and ζ is no longer negligible.

The correlation established with matrix-isolated gold atoms where Z_{eff} varies nearly linearly with polarizability is continued with silver (Figure 2b). Z_{eff} is calculated from the relationship

$$\Delta E(^2\mathrm{P}_{1/2} - {}^2\mathrm{P}_{3/2})\ \mathrm{cm}^{-1} = (921/(3.4)^4)(Z_{\mathrm{eff}})^4$$

In N_2 and D_2 matrices the crystal field splitting has increased compared to the noble gases just as in the case of Au, and the spin–orbit coupling follows the expected trend. In Ne, ζ is again smaller than observed in Ar but it is not reduced to the value in Xe as is the hyperfine coupling constant. $|A|$ is also small but not drastically reduced as in gold.

An interesting observation is that in neon the Ag atomic spectrum consists of five resolved absorptions which sharpen on annealing (Figure 3). These absorptions can be deconvoluted to give six peaks which form two groups of three absorptions each separated by a nearly constant difference. Together with the behavior of ζ and A the optical data strongly suggest that silver occupies at least two different sites in neon matrices.

Silver Dimers. In all experiments with silver atoms weaker features appear to higher and lower energies of the main absorptions. These have previously been attributed to silver dimers,[7,11] although correlation with gas-phase spectra[14,15] and theoretical calculations[11] have been tentative because the

Table II. Ag_2 Absorptions in Neon at 5 K

λ, nm	ν, cm^{-1}	Assignt (gas-phase T_e)
235.0 ± 0.5	42 535	
244.5	40 880	$E-X$ (40 159)
260.5	38 370	$D-X$ (39 023)
265.5	37 650	$C-X$ (37 626)
273.5	36 550	$B-X$ (35 827)
356.0	28 080	
380.0	26 310	
417.5	23 945	$A-X$ (22 996)

Table III. Ag_2 Absorptions in Argon with Temperature Dependent Shifts

λ, nm	ν, cm^{-1}	Temp dependence
237.5 ± 0.5	42 090	Observed only at 5 K
244.0	40 965	
259.5	38 520	
265.5	37 650	Shifts to 262.5 at 5 K
270.5	36 955	
280.5	35 640	Not observed at 5 K
383.0	26 100	Large intensity shift, strong at 20 K and weak at 5 K
408.0	24 505	Large intensity shift, weak at 20 K and strong at 5 K
440.0	22 720	

features are weak and poorly resolved. However, we have found in our experiments that by reducing the dilution ratio from 10^5:1 to 10^4:1 these features grow in intensity and can be resolved into a maximum of eight bands depending on the matrix.

Dimer formation appears to occur during formation of the matrix and not by diffusion after the matrix has formed or initially by sputtering dimers from the metal surface. This conclusion is based on the fact that annealing did not increase the intensity of the dimer bands while increasing M/R enhanced the dimer intensity relative to the atomic absorption features.

High M/R ratio experiments were done in both Ar and Ne matrices and, as is often the case, the molecular features are much sharper in Ne (Figure 4). It is also noted that in Ar there is a reversible temperature dependent shift in both band intensity and matrix position. The band position and assignments in Ne and Ar are listed in Tables II and III. The high-energy bands correlate well with the gas-phase spectra[14,15] as there are four known systems above 35 000 cm^{-1} and four strong absorptions in the matrix. Below 35 000 cm^{-1} there is only one reported gas-phase system, A → X, with T_e = 22 996 cm^{-1}. In the matrix below 35 000 cm^{-1} there are three distinct absorptions nonattributable to Ag atoms of which Ozin and Moskovits[11,12] report only the band at 26 180 cm^{-1} in Ar, and through careful quantitative metal atom concentration studies they assign this band to Ag_2. To assign this band to the A → X system requires a matrix shift of 3200 cm^{-1} which is quite large. It seems more reasonable to correlate the lowest energy band in both Ar and Ne with the A → X system. The correlation between the matrix bands at 28 080 (Ne) and 26 310 (Ne) cm^{-1} and the identified systems of Ag_2 at this time is not possible as no other gas-phase systems are known. It should be noted that no rotational analysis of the gas-phase spectra has been done and the lower states in each gas-phase system are assigned as the ground state because the system is seen in absorption and because the lower state vibrational constants are similar.

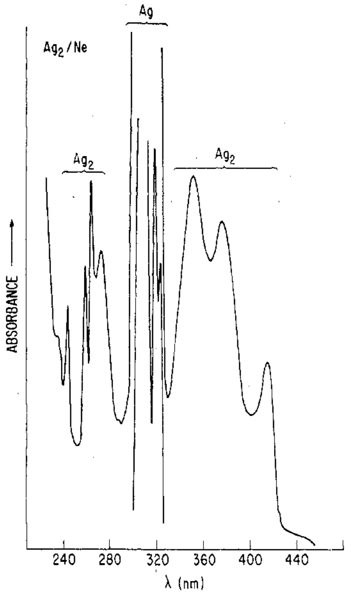

Figure 4. Absorption spectrum of silver dimers isolated in a Ne matrix.

Conclusion

From the relationship between Z_{eff} and polarizability it is clear that the model explaining the variation of the spin–orbit coupling with an increase in electron-charge density nearer the metal atom nucleus can be extended for Au atoms to include D_2 and N_2 matrices and appears to hold for silver atoms as well. The effects of site size and symmetry in D_2 and N_2 are to increase the crystal field splitting but not to substantially alter the dependence of spin–orbit coupling on polarizability.

In neon, where both the single substitution site size and polarizability are small, the metal atoms occupy multiple sites. This contention is supported by the parallel behavior of the spin–orbit and hyperfine coupling constants of both silver and gold atoms in noble gas matrices, by the discontinuity in the Z_{eff} vs. α plot for neon, and by the direct observation of splitting in the optical spectrum of silver in neon matrices.

Registry No. Au, 7440-57-5; Ag, 7440-22-4; Ag_2, 12187-06-3.

References and Notes

(1) Work performed under the auspices of the Division of Physical Research of the U.S. Energy Research and Development Administration.
(2) J. K. Bates and D. M. Gruen, *Rev. Sci. Instrum.*, **47**, 1506 (1976).
(3) (a) D. M. Gruen, S. L. Gaudioso, R. L. McBeth, and J. L. Lerner, *J. Chem. Phys.*, **60**, 89 (1974); (b) L. Brewer and B. King, *ibid.*, **53**, 3981 (1970).
(4) D. M. Kolb, F. Forstmann, D. Leutloff, and W. Schulze, *J. Chem. Phys.*, in press.
(5) D. M. Kolb and W. Schulze, *J. Chem. Phys.*, **64**, 2552 (1976).
(6) W. Schulze, D. M. Kolb, and H. Gerischer, *J. Chem. Soc., Faraday Trans. 2*, **71**, 1763 (1975).
(7) F. Schoch and E. Kay, *J. Chem. Phys.*, **59**, 718 (1973).
(8) J. S. Shirk and A. M. Bass, *J. Chem. Phys.*, **49**, 5156 (1968).
(9) L. Brewer, B. A. King, J. L. Wing, B. Meyer, and G. F. Moose, *J. Chem. Phys.*, **49**, 5209 (1968).
(10) P. H. Kasai and D. McLeod, *J. Chem. Phys.*, **55**, 1566 (1971).
(11) G. Ozin, *Appl. Spectrosc.*, **30**, 573 (1976).
(12) G. A. Ozin and M. Moskovits, "Cryochemistry", Wiley, New York, N.Y., 1976, Chapter 9.
(13) D. P. Strommen, D. M. Gruen, and R. L. McBeth, *J. Chem. Phys.*, **58**, 4078 (1973).
(14) J. Ruamps, *Ann. Phys. (Paris)*, **4**, 1111 (1959).
(15) C. Shim Piaw, W. Loong-Seng, and L. Yoke-Seng, *Nature (London)*, **209**, 1300 (1966).